LETTERS IN BIOMATHEMATICS
An International Journal

RESEARCH ARTICLE

OPEN ACCESS

Predictive QSAR and Molecular Docking Investigation of 1,3,4-Oxadiazoles with Pharmacokinetic Evaluation for Potent Transpeptidase Inhibition

B. Siva Kumar[1], L. Siva Shanker Reddy[2], Anwar Hussain[2], Jadigam Savithri[3], C. Madhusudhana Chetty[4], Vijey Aanandhi M1, K. Ilango[5], N. Yella Subbaiah[2]*

[1]School of Pharmacy, SBV Chennai, Sri Balaji Vidyapeeth (Deemed to be University), Puducherry – 607402, India
[2]Department of Pharmaceutical Chemistry, Santhiram College of Pharmacy, Nandyal – 518501, Andhra Pradesh, India
[3] Department of Pharmaceutical Chemistry, St. Jhon's College of Pharmaceutical Sciences, Yemmiganur.
[4] Department of Pharmaceutics, Santhiram College of Pharmacy, Nandyal – 518501, Andhra Pradesh, India
[5] Crescent School of Pharmacy, Chengalpattu (Dt), Tamil Nadu, India.
***Corresponding author**
Associate Professor, Department of Pharmaceutical Chemistry, Santhiram College of Pharmacy, Nandyal.
E-mail address: yellasubbaiah27@gmail.com (N. Yella Subbaiah)

ABSTRACT

In this QSAR study, a large dataset of 1,3,4-oxadiazole derivatives was encoded with a variety of chemical descriptors to create a statistically sound, stable, and predictive quantitative structure–activity relationship (QSAR) model aimed at the transpeptidase enzyme. The creation of this statistically validated model offers a viable foundation for investigating descriptor-based manipulation of transpeptidase inhibitory mechanisms. Multiple statistical factors were used to execute strict internal and external validations, which showed that the model was very reliable and not random. The validated QSAR model was subsequently utilized to forecast the biological activity of newly synthesized analogues, thereby pinpointing prospective lead compounds. To enhance the QSAR results, molecular docking simulations were performed on the highest-predicted active chemicals to clarify their binding orientations, interaction patterns, and structural compatibility within the enzyme's active site. Of the proposed series, chemicals M26 and M27 (after correcting for duplication) had the best docking scores of −8.90 and −9.44 kcal/mol, respectively. This means that they have a significant binding affinity and a strong ability to block the transpeptidase enzyme. These results suggest that the discovered compounds could function as viable scaffolds for the creation of novel antibacterial medicines and may signify a substantial progress in treatment techniques aimed at bacterial cell wall production. We did pharmacokinetic and drug-likeness tests (ADME profiling) to find out how well the developed compounds work and how well they can be absorbed by the body through the mouth. All of the compounds followed Lipinski's Rule of Five, which showed that they had good drug-like properties and could move on to preclinical testing. The results of QSAR modeling, molecular docking, and ADME analysis together show that the computational method is reliable and point to the 1,3,4-oxadiazole framework as a good structural motif for making new transpeptidase enzyme inhibitors.

ARTICLE HISTORY
Received September 17, 2026
Accepted October 28, 2026

KEYWORDS
QSAR, 1,3,4-oxadiazole derivatives, transpeptidase enzyme, molecular docking, ADME, drug-likeness, Lipinski's Rule of Five, enzyme inhibitors, antibacterial agents, computational modelling

1. Introduction

1,3,4- Oxadiazole

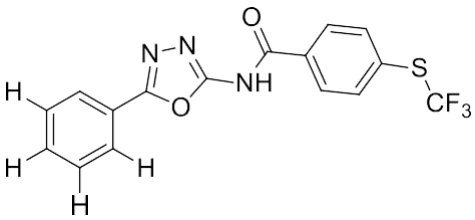
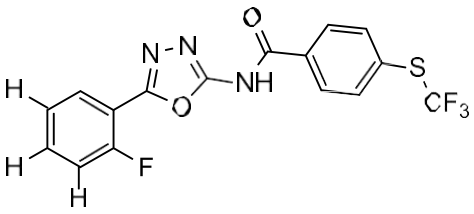
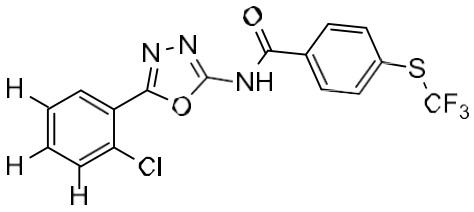
A heterocyclic moiety is typically present in freshly produced compounds, and motifs containing the 1,3,4-oxadiazole ring make up a sizable class of possible antibacterial derivatives. Five-membered heterocyclic compounds with one oxygen atom and two nitrogen atoms make up oxadiazoles. Several isomeric forms of oxadiazole, which are found in the structures of numerous medications, can be distinguished. The most promising structures are 1,3,4-oxadiazole derivatives. At the end of the nineteenth century, the first derivatives of 1,3,4-oxadiazole were prepared. The 1,3,4-oxadiazole ring influences the physicochemical and pharmacokinetic properties of the whole molecule. The 1,3,4-oxadiazole ring has also generated interest in medicinal chemistry as a carbonyl containing bio isostere like carboxylic acids, esters and amides. The oxadiazole ring is employed also as an important portion of the pharmacophore that can bind with a ligand. In other instances, it functions as a planar aromatic linker to provide optimal orientation of the molecule [1]. These aspects of the 1,3,4-oxadiazole ring have led to an extensive array of pharmaceutical uses of these molecule. As per literature, for several decades, scientists across the globe have been designing novel compounds bearing the 1,3,4-oxadiazole core, which possessed a broad range of biological

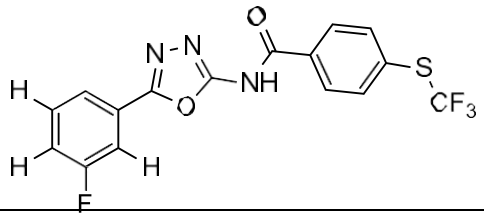
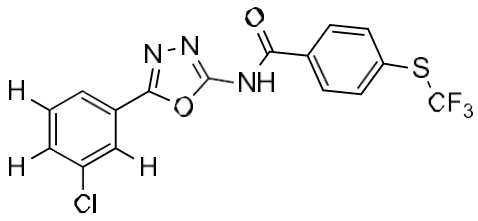
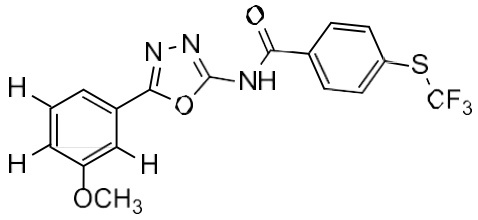
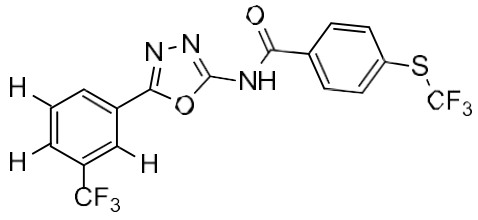
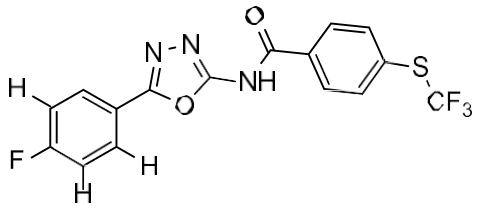
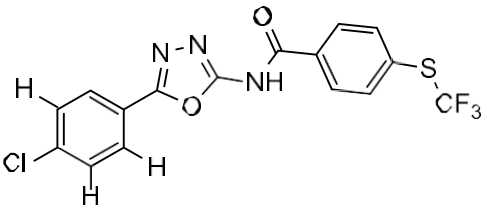
activity, such as anti-inflammatory [2.3,4,5], analgesic [6], anti-depressive [6,7], anticancer [8,9] and anti-diabetic [10,11] effect. Furthermore, there are also several literature reports supporting the general antimicrobial effect of compounds featuring the 1,3,4-oxadiazole ring in its structure. Researchers have reported investigations on antibacterial [12,13,14], antifungal [15,16] or antiviral [17,18] molecules with a 1,3,4-oxadiazole framework. Because of the extensive antimicrobial activity of 1,3,4-oxadiazole derivatives, in this review we would like to summarize the results of scientists during the past seven years. The review herein is based on publications from 2015 to 2021; the PubMed database was queried for literature, using the search words "1,3,4-oxadiazole", "antibacterial", "antitubercular", "antifungal", "antiprotozoal", "antiviral", and "activity". Compounds were classified by single antimicrobial activity; where applicable, a classification by chemical structure was also applied.

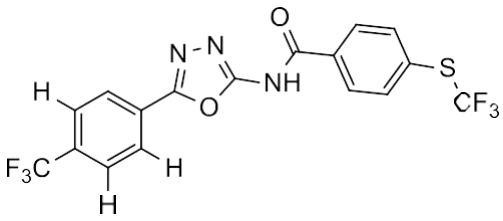
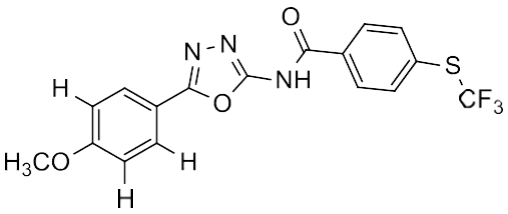
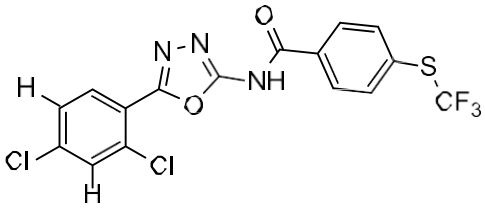
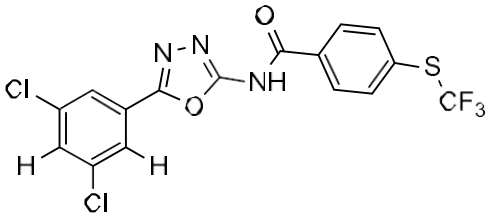
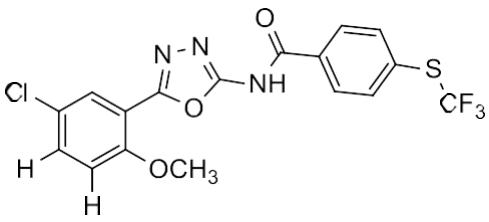
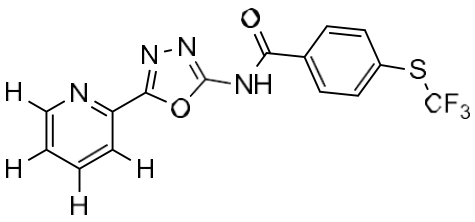
QSAR Models developed for 1, 3, 4 – Oxadiazole derivatives dataset

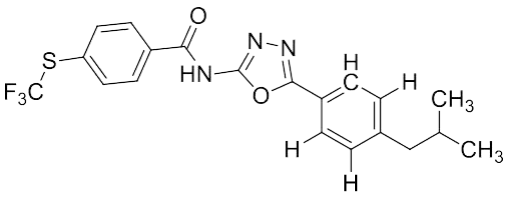
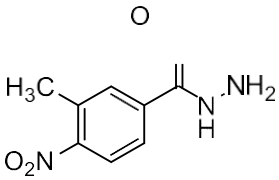
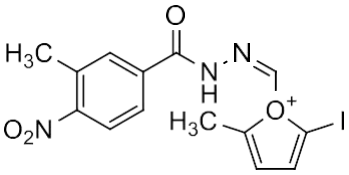
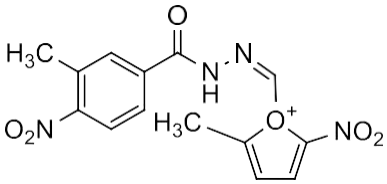
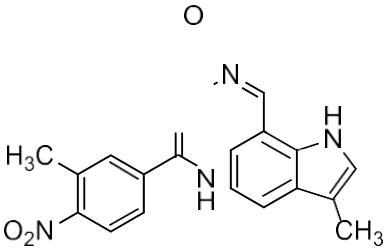
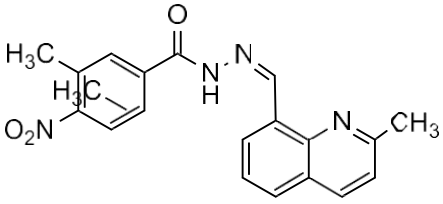
The dataset encompassing 60 compounds displayed in Table 1. with trans-peptidase inhibition values of 1,3,4 oxadiazole was congregated from published literature (Qin, J et.al, 2010) for the QSAR model construction **Table 1**. QSAR modelling for the selected dataset was investigated extensively using statistical tools and the molecular descriptors' information obtained was utilized for designing lead compounds thereof. Statistical criteria were used to validate the software settings of 'QSARINS' that were used to create MLR models using ordinary least squares. The QSAR model built for the 1,3,4 oxadiazole dataset must be cross validated (i.e., it must be robust) and evaluated for external validation (meaning predictability of bioactivity). The best models with QSARINS parameters are listed below

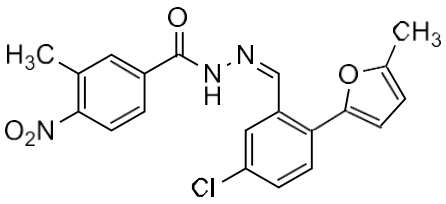
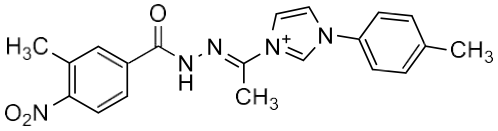
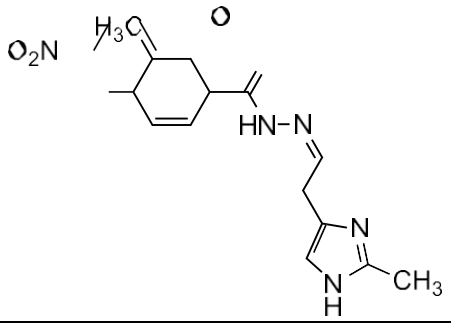
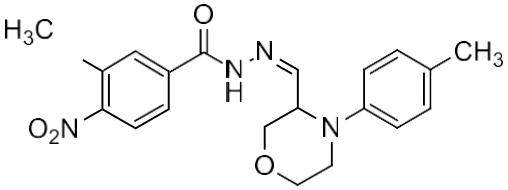
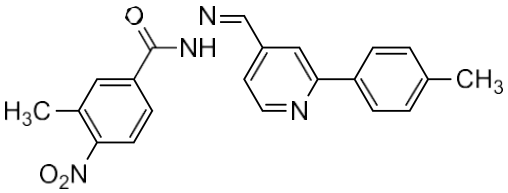
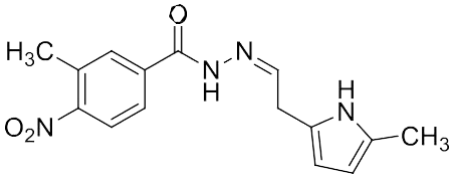
Table 1: MIC and PMIC Values of the Data Set Compounds

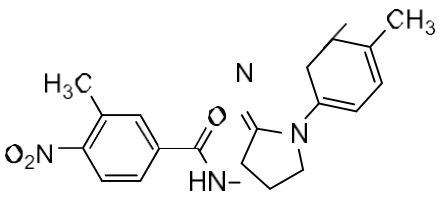
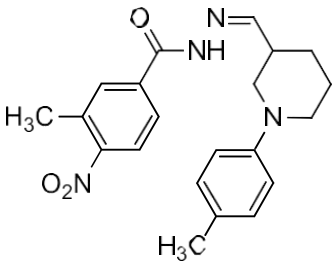
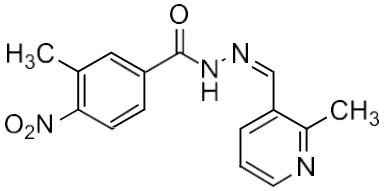
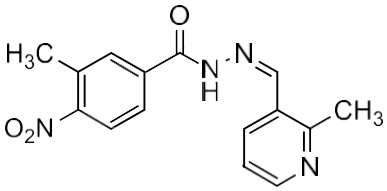
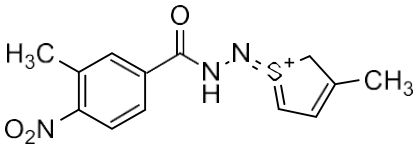
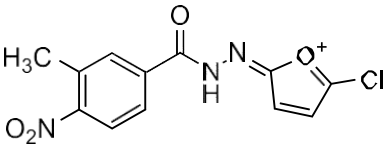
.NO.	STRUCTURE	MIC	PMIC
1		2	11.7389
2		4	0.11777
3		4	7.05289

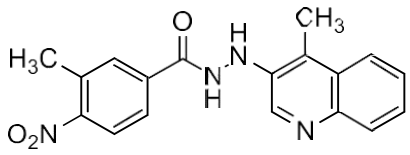
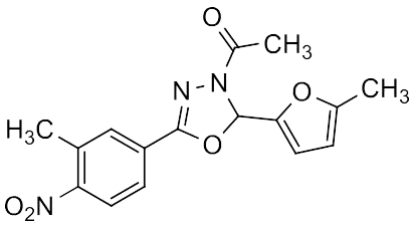
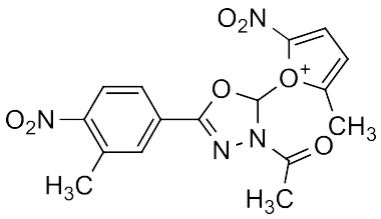
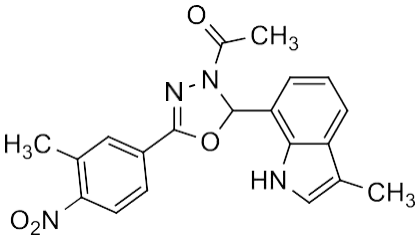
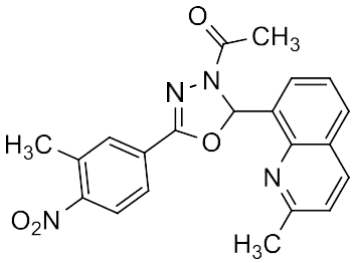
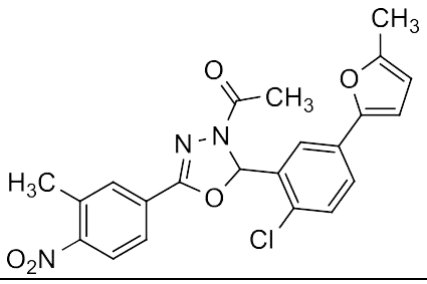
4		1.3	7.67563
5		1.3	6.40626
6		4	1.82701
7		1.5	7.45161
8		4	-1.88747
9		2	7.50689

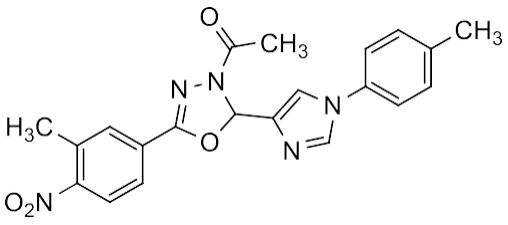
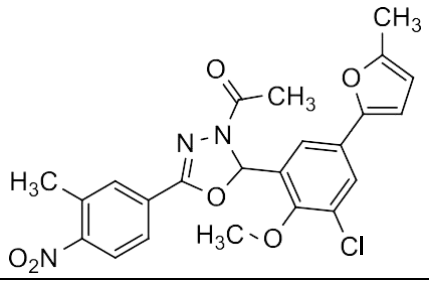
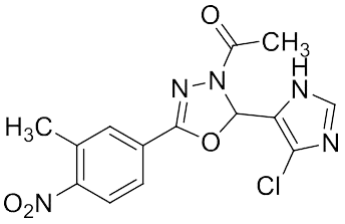
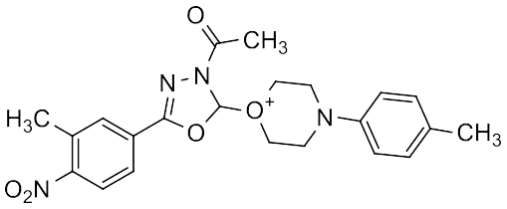
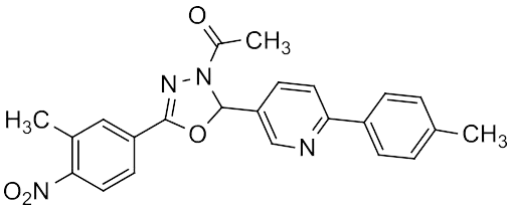
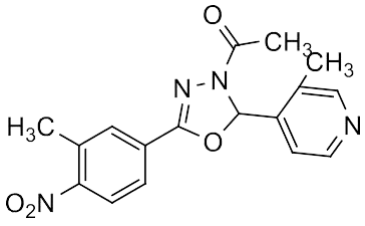
10		1.25	1.88879
11		4	7.71422
12		1.3	-0.43945
13		1.7	3.80493
14		2	4.56336
15		8	-4.43693

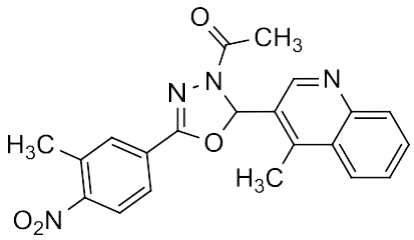
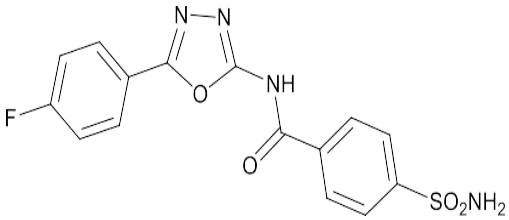
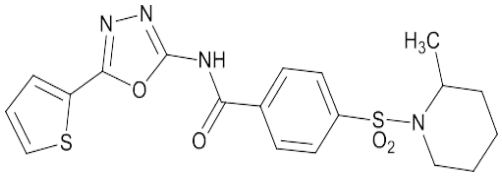
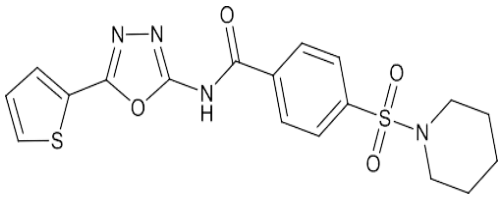
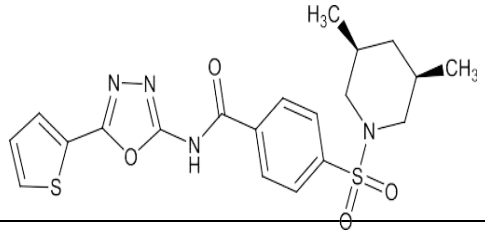
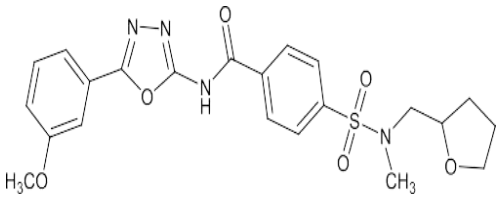
16		10	9.950966
17		15	19.21609
18		10	17.39016
19		50	13.42221
20		10	9.950966
21		10	34.66141

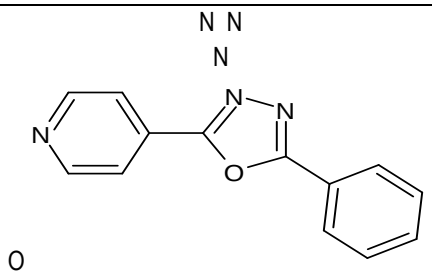
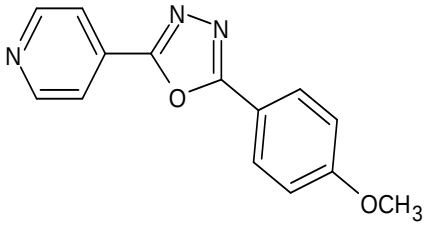
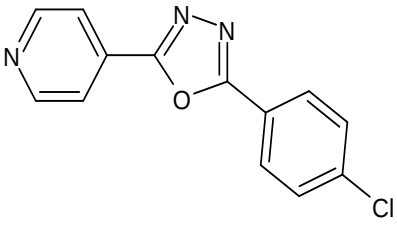
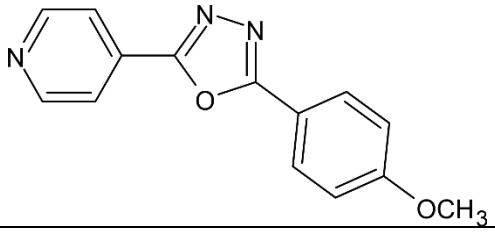
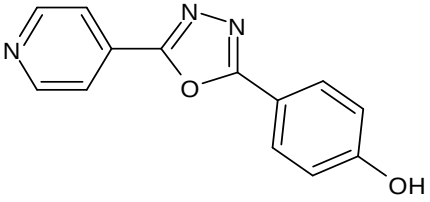
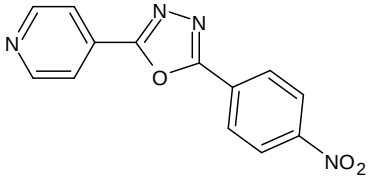
22		10	15.19673
23		10	25.11221
24		10	19.09556
25		10	16.53467
26		50	2.817047
27		10	23.84149

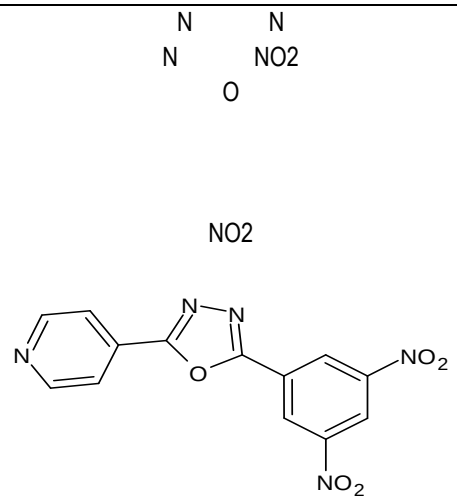
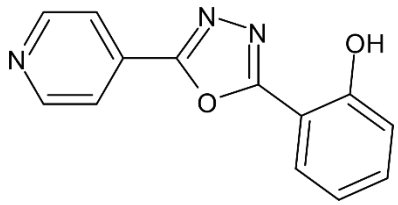
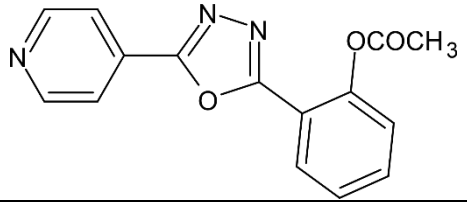
28		50	23.12731
29		50	21.01631
30		10	10.42203
31		10	1.831611
32		10	33.68276
33		50	12.30417

34		50	22.77312
35		15.62	21.72235
36		10	21.0296
37		10	17.18757
38		10	29.98087
39		50	15.56946

40		10	20.92146
41		10	40.65611
42		10	8.48574
43		10	19.26375
44		10	17.98103
45		10	20.08154

46		15.62	40.66
47		16	8.486
48		8	19.26
49		16	17.98
50		2	20.08
51		32	17.81

52		52	7.334037
53		81	20.44574
54		68	10.35023
55		77	7.297335
56		86	29.46596
57		46	37.66076

58		48	79.38799
59		59	77.17703
60		83	76.19976

Pre-treatment and division of data set:

Utilizing Data Pre-treatment Software GUI 1.2, the descriptor matrix acquired from the CHEMOPY server was refined to exclude constant, near-constant, and extraneous molecular descriptors, thereby improving the quality and resilience of the dataset. Subsequently, the Kennard–Stone technique was utilized to methodically partition the dataset into 27 calibration (training) compounds and 12 validation (test) compounds, guaranteeing a consistent distribution of structural diversity in both sets. The stratified partitioning enabled the creation of a dependable and statistically significant quantitative structure–activity relationship (QSAR) model, depicted by a mathematical correlation equation linking chemical descriptors to biological activity.

QSAR formula:

A quantitative structure–activity relationship (QSAR) model was constructed using the Lack of Fit (LOF) function in the QSARINS software environment. In this model, the anti-proliferative activities represented by pMIC values were treated as the dependent variable, whereas the chosen molecular descriptors acted as the independent variables. To guarantee the strength and predictive accuracy of the developed model, an external validation set—consisting of compounds not used in the model-building or internal validation stages—should be utilized to evaluate the model's predictive performance and ability to generalize.

Model validation:

Models developed using "QSARINS" were evaluated for applicability and internally and externally validated. Selected models underwent the use of external validation the $Q_2\ F_1$, $Q_2\ F_2$, and $Q_2\ F_3$ techniques, concordance correlation coefficient (CCC), internal validation using the Cross-validation leave-one-out (Q_{2LOO}), Cross-validation leave-many-out (Q_{2LMO}), Root mean squared error (RMSE),

and Y-scrambling techniques. During the 5000 Q_{2LMO} runs, 50% of the training set's objects are removed. Y-scrambling aims to eliminate chance association in the initial model by rearranging answer data across 5000 iterations. It is crucial to remember that the R^2 and Q_{2LOO} should be more significant than the more fantastic scrambled ones and that the model's RMSE under prediction should have a lower RMSE.

Since it measures the consistency between two variables, the CCC (CCC_{ext}) is a tool used to analyze the repeatability of models. Using leverage analysis, the descriptors employed and evaluated establish the theoretical area modeling's applicability domain.

Stepwise regression, fitting with successive additions of descriptors, significantly improved the fit when the model could no longer be improved, and then the descriptors that had the most negligible statistically significant impact on model fit were dropped. The process was repeated until no more descriptors could be deleted without suffering a statistically significant fit loss. Three models were made using these criteria. With the fewest descriptors, the highest (R^2) was found with no descriptor co-linearity and the best prediction model was selected for future development, as provided in **Table 2**. The models' validity was evaluated using the "leave-one-out" (LOO) cross-validation technique. During the validation step, the model function is trained using data from every molecule but one. The pMIC for the chemical that was not a part of the study was then predicted using the model's properties. They utilize statistical measures like Q_2 (cross-validated correlation coefficient), R^2 (regression coefficient), SD (standard deviation), and SE (standard error) in the proposed QSAR models. The least necessary values for evaluating the mathematical equation are listed in **Table 2**. The table parameters adjusted the derived equations' effectiveness and predictive capability.

ADME and drug-likeness predictions:

To ascertain their pharmacological similarity, the best-fitting ligands obtained by molecular docking were through ADME analysis. The ADME forecasts were created using a web application called Swiss ADME. A few characteristics (HIA) were Lipophilicity LogP, molar solubility in water LogS, BBB permeability, skin permeation, and human gastrointestinal absorption. The synthetic accessibility was predicted using a score from 1 to 10, where one indicates that the synthetic route is fairly pretty forward and ten indicates that the substance's structure is complex and that it is challenging to synthesize, along with such as Lipinski's rule of five, which have drug-like qualities. In addition, the bioavailability score was computed. Using the toxicity prediction, the possible toxicity of the inhibitors was estimated.

On Chemdraw Ultra 16.0, the recommended compounds' 2D structures were created to analyze their pharmacokinetic characteristics. When each structure was imported, the structural grin was entered into the (http://swissadme.ch/) interface. The ADMET features and criteria were produced by the Swiss ADME drug design study. The receptor transpeptidase enzyme inhibitor, was used in molecular docking experiments on five drugs with significant pMIC. The ligand (compounds) were also converted to PBD format as indicated in Figure 1 (Receptor and Ligand 3D structures and the receptor was retrieved from Protein Data Bank (Code: 5L3J and 3FV5) and set using Discovery Studio software. To determine the binding affinity of the ligand and receptor, Autodock version 4.2.6 was used.

2. Results and Discussion

QSAR model developed and designed structures:

Sixty 1,3,4-oxadiazole derivatives (Compounds 1–60) were assessed as transpeptidase enzyme inhibitors according to pharmacological data documented in the literature. The antimicrobial activity of these compounds was quantified using pMIC values, derived from the minimum inhibitory concentration (MIC), which represents the concentration of a compound required to inhibit 30% of microbial growth under standardized experimental conditions.

Principal Component Regression (PCR) and Partial Least Squares Regression (PLS) studies were used to ascertain a link between biological activity (pMIC) and molecular descriptors, aiming to identify potential linear associations. The Multiple Linear Regression (MLR) model demonstrated greater predictive ability among the constructed statistical models, evidenced by a higher coefficient of determination (R^2) and a minimal number of predictive descriptors. This demonstrates that the MLR method successfully identified the most critical chemical factors affecting the transpeptidase inhibitory action of the 1,3,4-oxadiazole derivatives.

QSAR EQUATION

Model 1

pIC_{50} = 80.543+(-5.4233)*(DS) +(-23.8311)*(MoRSEP8) +(-4.3233)*(L2v)+(-29.4801)* (RDFC7) n_{tr} = 60 npred = 30 R^2=0.7895 R^2adj= 0.7708 R^2-R^2adj = 0.0187 LOF = 168.3286 Kxx = 0.2172 Delta K = 0.01133 $RMSE_{tr}$ = 10.8983 MAE_{tr} = 8.3401 RSS_{tr} = 5938.6341 CCC_{tr} = 0.8824 s = 11.4878 F =42.1879 Q2loo = 0.7500 R^2-Q2loo = 0.0394 $RMSE_{cv}$ = 11.8752 MAE_{cv} = 9.2092 $PRESS_{cv}$ = 7050.9676 CCC_{cv} = 0.8600 $Q2_{LMO}$ = 0.7335 R^2_{Yscr} = 0.0802 $Q2_{Yscr}$ = -0.1461 $RMSEAV_{Yscr}$ = 22.7702 $RMSE_{ext}$ =13.9088 MAE_{ext} = 11.1394 $PRESS_{ext}$

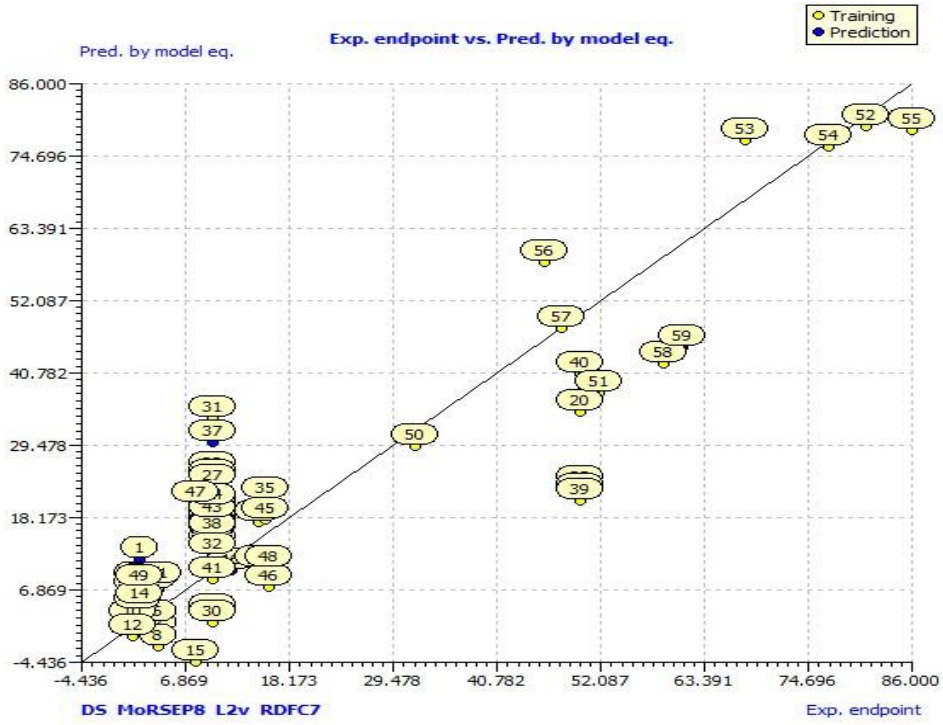
= 1741.0941 R^2ext = 0.5196 Q2-F1 = 0.5139 Q2-F2 = 0.5079 Q2-F3 = 0.6571 CCC_{ext} = 0.6449 r2m aver = 0.3508 r2m delta = 0.2697

Model 1 showed a strong fit and yielded acceptable results in internal validation. The lack of outliers in the William's plot supports the dataset's reliability; however, a minor reduction in external validation parameters was noted relative to the prior model. The correlation matrix for Model 1, accompanied by the scatter plot illustrating the inhibitory activities of 1,3,4-oxadiazole derivatives on the transpeptidase enzyme, demonstrates a robust linear relationship between predicted and observed values. The plot of Kxy (inter-correlation between descriptors and response) against Q^2LMO demonstrates that the model exhibits robustness and stability, as the "leave-many-out" (LMO) cross-validation parameters closely align with the original model statistics.

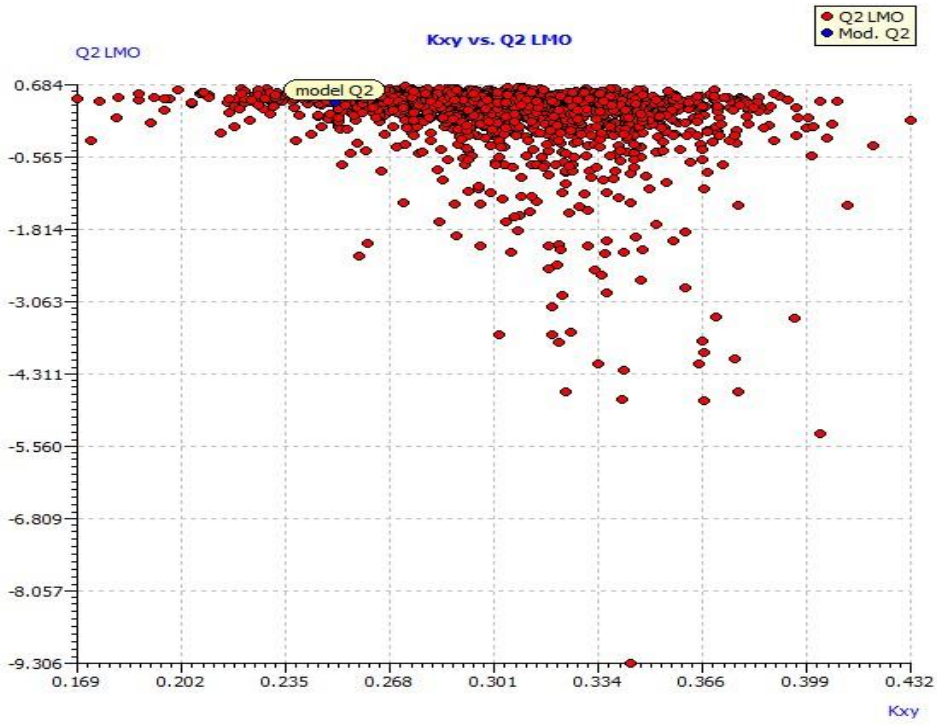
The structural–activity relationship is upheld, demonstrated by the notably higher correlation coefficients (R^2 and Q^2) of the final model in comparison to those derived from endpoint scrambling. Figure 4 illustrates the Y-scrambling plot of Kxy against R^2Yscr and Q^2Yscr, demonstrating that the obtained model is not attributable to random correlation. The applicability domain, as depicted in the William's plot of standardized residuals against leverage values (Figure 6), indicates that all compounds exhibit leverage values beneath the critical threshold (h = 0.462), thereby confirming that all data points reside within the model's reliable prediction space.

The external validation parameters—Q^2F1, Q^2F2, and Q^2F3—showed similar and consistently high values, and the concordance correlation coefficient (CCC) indicated a robust predictive alignment between experimental and theoretical data. The results collectively confirm that the developed model is not a product of random correlation, indicating a significant relationship between the structural features of 1,3,4-oxadiazoles and their inhibitory potential toward the transpeptidase enzyme.

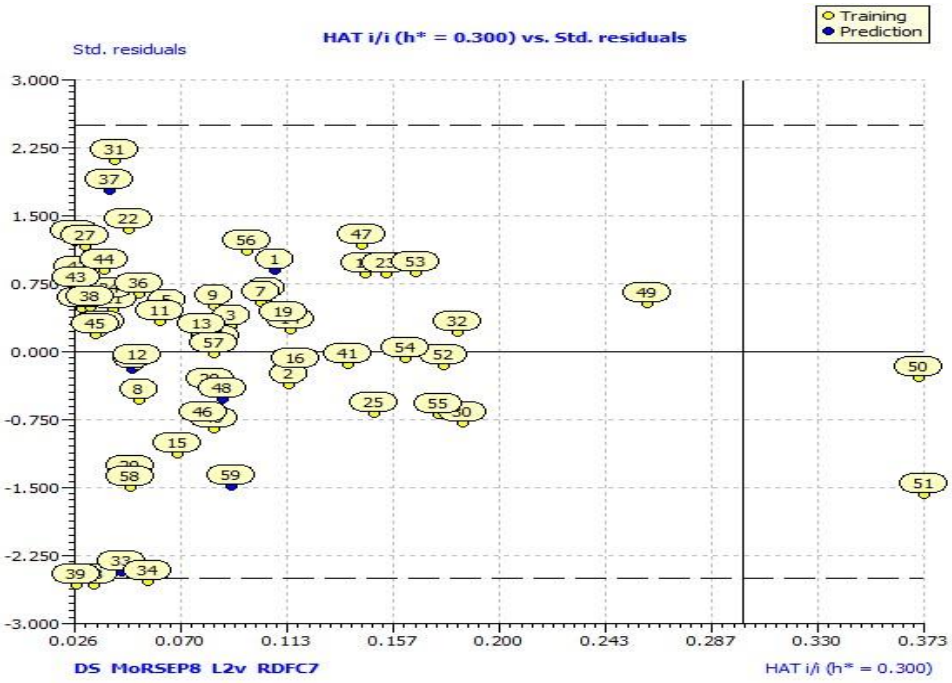
At the molecular level, the distribution of partial atomic charges is essential in influencing interatomic distances and electronic interactions among atoms with differing electron densities. With an increase in scattering parameters, the three-dimensional MoRSEC1 descriptors, weighted by hydrogen-lighter schemes, exhibit diminished variability, indicating stable electrostatic and steric contributions throughout the dataset. Conversely, descriptors influenced by atomic mass, van der Waals volume, and polarizability exhibit comparatively minor variations, aligning with findings from prior literature. This indicates that electronic factors play a more substantial role than steric or mass-related properties in the observed biological activity.



Scatter diagram of dataset compounds based on testing results of the best model equation



Visualization of dataset compounds using LMO scatter plots based on experimental values from the best model equation



The best model plot by William (h*, 0.455) warning value

ADME Properties:

A number of important physicochemical and pharmacokinetic properties of the recently created compounds were identified by the ADMET analysis, providing important information about their potential as oral active treatments. Critical chemical descriptors and adherence to the "Rule of Five," which together characterize the drug-likeness and bioavailability of small compounds, were among the

evaluated factors. The octanol–water partition coefficient (iLOGP), molecular weight (MW), number of rotatable bonds (RB), hydrogen bond donors (HBD), hydrogen bond acceptors (HBA), number of heavy aromatic atoms (nAH), molecular refractivity (MR), and topological polar surface area (TPSA) were among these metrics.

All of the synthesized 1,3,4-oxadiazole derivatives, as listed in Table 6, demonstrated physicochemical characteristics that fell within the permissible bounds established by Lipinski's Rule of Five, suggesting good oral bioavailability and permeability. The fact that none of the compounds failed to meet more than one Lipinski criterion indicates that they have drug-like properties appropriate for additional pharmacological and in vivo testing. The equilibrium between hydrophilic and lipophilic characteristics, which is necessary for effective membrane transport and receptor binding, is further supported by the measured iLOGP and MR values. The developed compounds' potential as lead candidates for transpeptidase enzyme inhibition is highlighted by these ADMET results, which collectively imply that they are structurally compliant, pharmacokinetically compatible, and chemically stable in accordance with accepted principles of rational drug design.

Table 2: .Best Model Equation Predicted PMIC Values of the Original DataSet

Compound Code	MIC	DS	MORSE – P8	L2V	RDFC7	PMIC	RESIDUAL
M1	2	16.66	-1.334	2.601	-0.034	11.73893	-9.73893
M2	4	18.076	-1.258	3.087	-0.033	0.117769	3.882231
M3	4	16.692	-1.176	2.692	-0.022	7.052889	-3.05289
M4	1.3	17.597	-1.467	3.61	-0.109	7.675632	-6.37563
M5	1.3	16.688	-1.352	4.56	-0.131	6.406262	-5.10626
M6	4	16.711	-1.001	3.601	-0.123	1.827014	2.172986
M7	1.5	17.332	-1.182	2.621	-0.138	7.451609	-5.95161
M8	4	17.298	-1.081	4.308	-0.144	-1.88747	5.887466
M9	2	16.684	-1.034	2.578	-0.134	7.506886	-5.50689
M10	1.25	17.066	-1.361	5.344	-0.155	1.88879	-0.63879
M11	4	16.705	-1.344	4.683	-0.203	7.714218	-3.71422
M12	1.3	16.716	-1.118	4.798	-0.128	-0.43945	1.739454
M13	1.7	16.715	-0.944	2.722	-0.108	3.804927	-2.10493
M14	2	16.746	-1.036	2.217	0.009	4.563361	-2.56336
M15	8	16.661	-1.118	4.987	-0.01	-4.43693	12.43693
M16	12	16.742	-1.083	2.06	-0.112	9.950966	2.049034
M17	10	11.541	-0.328	1.809	-0.043	19.21609	-9.21609
M18	15	12.445	-0.816	3.385	0.016	17.39016	-2.39016
M19	10	12.569	-0.43	2.19	-0.009	13.42221	-3.42221
M20	50	12.611	-1.38	2.959	-0.082	34.66141	15.33859

M21	10	12.657	-0.868	4.329	-0.045	15.19673	-5.19673
M22	10	12.748	-1.332	4.179	-0.001	25.11221	-15.1122
M23	10	12.747	-1.217	6.445	-0.222	19.09556	-9.09556
M24	10	12.362	-0.806	3.966	-0.033	16.53467	-6.53467
M25	10	12.743	-0.618	5.802	-0.059	2.817047	7.182953
M26	10	12.663	-1.083	4.073	-0.128	23.84149	-13.8415
M27	10	12.37	-1.095	3.99	-0.028	23.12731	-13.1273
M28	50	12.779	-0.776	3.141	-0.165	21.01631	28.98369
M29	15	12.693	-0.767	5.152	-0.092	10.42203	4.577966
M30	10	12.429	-0.176	2.61	0.143	1.831611	8.168389
M31	10	12.735	-0.997	2.787	-0.356	33.68276	-23.6828
M32	10	12.449	-0.117	2.749	-0.284	12.30417	-2.30417
M33	50	12.317	-0.718	2.749	-0.129	22.77312	27.22688
M34	50	12.735	-0.781	2.249	-0.046	21.72235	28.27765
M35	15.62	12.622	-1.009	4.176	-0.1	21.0296	-5.4096
M36	10	13.231	-1.233	4.499	0.052	17.18757	-7.18757
M37	10	12.915	-1.347	3.342	-0.062	29.98087	-19.9809
M38	10	13.017	-0.834	4.047	-0.11	15.56946	-5.56946
M39	50	13.157	-1.134	4.103	-0.083	20.92146	29.07854
M40	50	12.966	-1.596	3.286	-0.224	40.65611	9.343894
M41	10	13.379	-1.142	6.22	-0.006	8.48574	1.51426
M42	10	12.695	-0.881	3.46	-0.052	19.26375	-9.26375
M43	10	12.909	-0.902	3.529	-0.041	17.98103	-7.98103
M44	10	12.928	-1.013	4.654	-0.191	20.08154	-10.0815
M45	15.62	12.651	-0.791	3.26	-0.038	17.80952	-2.18952
M46	16	12.976	-0.846	5.033	0.042	7.334037	8.665963
M47	8	16.734	-1.186	5.154	-0.837	20.44574	-12.4457
M48	16	16.451	-1.013	5.329	-0.608	10.35023	5.649769
M49	2	16.191	-0.254	4.305	-0.92	7.297335	-5.29733

M50	32	16.548	-0.659	3.519	-1.295	29.46596	2.534037
M52	52	16.493	-1.516	6.021	-1.237	37.66076	14.33924
M53	81	5.1	-1.329	1.659	-0.068	79.38799	1.612006
M54	68	5.159	-1.238	1.963	-0.122	77.17703	-9.17703
M55	77	5.356	-1.251	1.659	-0.07	76.19976	0.800236
M56	86	5.177	-1.369	1.936	-0.07	78.78505	7.21495
M57	46	9.012	-1.318	1.675	-0.08	58.19449	-12.1945
M58	48	11.044	-1.29	1.689	-0.124	47.74367	0.256328
M59	59	11.621	-1.271	2.547	-0.187	42.30949	16.69051
M60	61	11.534	-1.395	1.796	-0.046	44.82648	16.17352

Table 3: Best model descriptors for the newly designed compound

COMPOUND CODE	DS	MORSEP8	L2V	RDFC7	PMIC
M1	16.66	-1.125	1.262	-0.012	11.8986
M2	18.076	-1.186	1.417	0.028	3.82356
M3	16.692	-1.073	1.327	0.029	8.99611
M4	17.597	-0.889	1.458	-0.041	1.20035
M5	16.688	-1.02	1.46	-0.044	9.3318
M6	16.711	-1.089	1.442	0.031	8.71822
M7	17.332	-1.034	1.469	-0.113	8.16805
M8	17.298	-1.389	1.597	-0.043	14.1955
M9	16.684	-0.813	1.934	-0.011	1.39837
M10	17.066	-3.325	0.899	-0.085	65.8465
M11	16.705	-1.19	1.862	0.056	8.60491
M12	16.716	-1.024	1.759	0.044	5.38835
M13	16.715	-1.041	1.894	0.048	5.09734
M14	16.746	-1.13	1.853	0.02	8.05288
M15	16.661	-1.255	1.467	0.029	12.8962

M16	16.742	-1.0939	0.969	-0.117	15.0749
M17	11.541	-2.8	1.02	-0.077	78
M18	12.445	-1.295	2.489	-0.033	34.1235
M19	12.569	-1.052	2.569	0.005	26.1939
M20	12.657	-1.122	1.728	-0.027	31.9641
M21	12.657	-1.16	1.883	-0.076	33.6441
M22	12.748	-0.777	2.628	-0.013	18.9452
M23	12.747	-0.878	1.585	-0.042	26.7216
M24	12.362	-0.974	1.589	-0.046	31.198
M25	12.743	-0.874	1.214	0.001	26.9843
M26	11.514	-3.2	1.422	0.077	85.9409
M27	12.37	-0.957	2.225	-0.056	28.2947
M28	12.779	-1.948	2.325	-0.075	49.821
M29	12.693	-1.073	3.084	-0.099	26.8613
M30	12.429	-2.829	1.78	-0.128	76.633

Table4: Predicted Physicochemical and Drug-Likeness Properties of the designed 1,3,4-thiadiazole derivatives.

Compound Code	MW(g/ mol)	M log P	HBA	HBD	MR	TPSA	nRot	Lipinski's rule (Ro5)	Veber rule
M1	257.253	1.171	6	2	73.81	107.995	3	+	+
M2	227.227	1.7089	5	2	68.66	96.516	2	+	+
M3	261.672	2.3623	5	2	72.33	106.82	2	+	+
M4	261.672	2.3623	5	2	72.33	106.82	2	+	+
M5	245.217	1.848	5	2	67.28	100.682	2	+	+
M6	245.217	1.848	5	2	67.28	100.682	2	+	+
M7	272.224	1.6171	7	2	76.14	111.169	3	+	+
M8	243.226	1.4145	6	3	69.34	101.311	2	+	+
M9	257.253	1.7175	6	2	73.81	107.995	3	+	+

M10	257.253	1.7175	6	2	73.81	107.995	3	+	+
M11	257.253	1.171	6	2	73.81	107.995	3	+	+
M12	227.227	1.7089	5	2	68.66	96.516	2	+	+
M13	261.672	2.3623	5	2	72.33	106.82	2	+	+
M14	261.672	2.3623	5	2	72.33	106.82	2	+	+
M15	245.217	1.848	5	2	67.28	100.682	2	+	+
M16	245.217	1.848	5	2	67.28	100.682	2	+	+
M17	272.224	1.6171	7	2	76.14	111.169	3	+	+
M18	243.226	1.4145	6	3	69.34	101.311	2	+	+
M19	257.253	1.7175	6	2	73.81	107.995	3	+	+
M20	257.253	1.7175	6	2	73.81	107.995	3	+	+
M21	291.108	2.8892	4	1	65.02	105.044	2	+	+
M22	325.553	3.5426	4	1	78.81	115.347	2	+	+
M23	325.553	3.5426	4	1	78.81	115.347	2	+	+
M24	309.098	3.0283	4	1	73.76	109.21	2	+	+
M25	309098	3.0283	4	1	73.76	109.21	2	+	+
M26	336.105	2.7974	6	1	86.62	119.697	3	+	+
M27	307107	2.5948	5	5	75.82	109.838	2	+	+
M28	321.134	2.8978	5	1	75.51	116.523	3	+	+
M29	321.134	2.8978	5	1	71.51	116.523	3	+	+
M30	321.134	2.8978	5	1	71.51	116.523	3	+	+

	absorption		distribution		metabolism							excretion	toxicity	
	Intestinal hum	Ds hum	BB permeability	CNS permeability	substrate		inhibitors					Total clearance	AMES toxicity	hepatotoxicity
					D6	A4	A2	C19	C9	D6	A4			
	Numeric% absorbed	Numeric (log|kg-l)	Numeric (log BB)	Numeric (log PS)	Category(yes/no)							Numeric (log ml/min/kg)	Category (yes/no)	
1	9.923	0.031	1.395	-2.986	es	o	es	es	o	o	es	0.636	es	es
2	0.308	0.392	1.218	-3.342	o	es	es	es	o	o	o	0.633	es	es
3	9.348	.037	1.376	-2.605	es	o	es	es	o	o	o	0.532	es	es
4	9.359	.046	1.361	-2.605	es	o	es	es	o	o	o	0.602	es	es
5	8.463	.42	1.399	-2.758	es	o	es	es	o	o	es	0.564	es	es
6	8.493	.058	1.421	-2.758	es	o	es	es	o	o	es	0.535	es	es
7	5.131	.031	1.416	-2.932	o	o	es	es	o	o	o	0.324	es	o
8	1.895	.055	1.374	-2.909	es	o	es	es	o	o	o	0.6	es	es
9	7.785	0.012	1.403	-2.999	es	o	es	es	o	o	es	0.584	es	es
10	2.883	0.035	1.411	-2.998	es	o	es	es	o	o	es	0.593	es	es
11	4.541	0.288	0.802	-2.602	o	es	es	o	o	o	o	0.157	es	es
12	5.671	0.318	0.954	-3.335	o	es	es	o	o	o	o	0.084	es	es
13	5.562	0.296	1.003	-3.346	o	es	es	o	o	o	o	0.133	es	es
14	0.742	0.391	1.035	-3.385	o	es	es	o	o	No	o	0.097	es	es
15	3.425	0.356	0.986	-2.619	o	es	es	o	o	o	o	0.084	es	es
16	9.405	.054	0.899	-2.792	o	o	es	es	o	o	o	-0.07	es	o
17	4.495	0.218	1.425	-3.477	o	o	es	o	o	o	o	-0.146	es	es
				-								0		

18	1.513	0.342	0.997	2.744	o	e	es	o	o	o	o	.138	es	es
19	1.67	0.404	1.018	-3.411	o	es	es	o	o	o	o	0.13	es	es
20	8.856	0.402	1.042	-3.403	o	es	es	o	o	o	o	0.168	es	es
21	2.093	0.352	0.788	-3.26	o	o	es	o	o	o	o	0.494	es	es
22	8.525	.701	.333	-2.08	o	o	es	o	o	o	es	0.408	es	o
23	8.813	.722	0.901	-2.08	o	o	es	o	o	o	es	0.477	es	o
24	9.715	.716	0.934	-2.33	o	o	es	o	o	o	es	0.44	es	o
25	9.859	.718	0.981	-2.33	o	o	es	o	o	o	es	0.411	es	o
26	8.112	.692	1.253	-2.407	o	o	es	o	o	o	es	0.25	es	o
27	7.589	.743	1.335	-2.834	o	o	es	o	o	o	es	0.476	es	o
28	1.883	0.371	0.982	-3.294	o	o	es	o	o	o	o	0.482	es	es
29	1.883	0.371	0.982	-3.294	o	o	es	o	o	o	o	0.482	es	es
30	1.883	0.371	0.982	-3.294	o	o	es	o	o	o	o	0.482	es	es

Predicted Pharmacokinetic (ADMET) Properties of the 1,3,4-thiadiazole derivatives

Molecular docking study

The three-dimensional crystal structures of the transpeptidase enzyme complexed with inhibitors (PDB IDs: 3FY8 and 3SRQ) at a high resolution of 1.95 Å were retrieved from the Protein Data Bank (RCSB; https://www.rcsb.org/). Prior to molecular docking, the protein structures underwent a comprehensive pre-docking optimization and refinement process using AutoDock 4.2.6 and BIOVIA Discovery Studio software suites. To prepare the receptor for docking, all crystallographic water molecules, heteroatoms, and co-crystallized ligands were meticulously removed to ensure a ligand-free binding pocket. Subsequently, polar hydrogen atoms were added, and Gasteiger–Marsili partial atomic charges were assigned using the MGL Tools package. The refined receptor structures were then saved in PDBQT format for docking simulation. The ligand molecules were designed and constructed using ChemDraw Ultra 16.0, followed by geometric and energy minimization using the MM2 force field in Chem3D to achieve the most stable conformers. The rotatable bonds of the ligands were defined to enable torsional flexibility, and the final ligand structures were saved in PDBQT format. During the docking process, the receptor structure was treated as a rigid macromolecule, whereas the ligands were considered flexible entities to allow conformational adaptation within the binding cavity. A grid box was generated to encompass all key amino acid residues constituting the enzyme's active binding site, ensuring comprehensive exploration of potential binding orientations. The grid dimensions were defined as 60 Å × 60 Å × 60 Å with a grid point spacing of 0.495 Å, centered at coordinates (x = 14.466589, y = 27.731196, z = 15.048571) for PDB 3FY8, and (x = 24.730461, y = 11.776095, z = 39.185090) for PDB 3SRQ, respectively. The Lamarckian Genetic Algorithm (LGA), a hybrid evolutionary optimization technique implemented in AutoDock 4.2.6, was employed to identify the most energetically favorable binding conformations. The population size was set to 150, and the maximum number of energy evaluations was defined as 25,000,000 to ensure exhaustive conformational sampling. The resulting docking poses were evaluated based on their binding free energy (ΔGbind) and inhibition constant (Ki) values. Post-docking analyses, including hydrogen bonding, hydrophobic interactions, electrostatic contacts, and π–π stacking, were visualized and interpreted using BIOVIA Discovery Studio Visualizer. These analyses provided insights into the binding orientation, molecular interactions, and stability of ligand–enzyme complexes, thereby validating the molecular docking outcomes.

Preparation of Ligand:

The synthesized 1,3,4-oxadiazole derivatives were formulated according to their specific chemical scaffolds utilizing ChemDraw Ultra 16.0 software to provide accurate two-dimensional illustrations. Subsequently, a variety of 1,3,4-thiadiazole analogues were modeled and protonated using BIOVIA Discovery Studio to confirm suitable ionization states at physiological pH. The synthesized molecular structures underwent geometry optimization and energy minimization utilizing the Molecular Mechanics Force Field (MMFF94) alongside the steepest descent algorithm. This technique facilitated the achievement of the lowest energy conformations, reducing steric strain and producing geometrically stable structures for subsequent study. AutoDock version 4.2.6 was utilized for molecular docking studies to assess the interaction patterns between the synthesized ligands and the target receptor. The docking simulations aimed to ascertain the binding affinities, interaction energies, and favored conformational orientations of the ligands within the receptor's active region. The obtained docking scores and binding conformations offered essential insights into the prospective inhibitory mechanisms and structure–activity connections of the synthesized 1,3,4-oxadiazole and 1,3,4-thiadiazole derivatives.

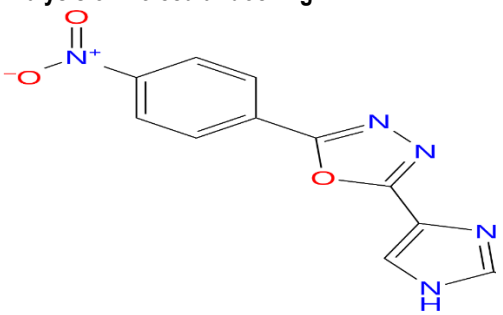
Molecular docking results for designed compounds using 3FY8

COMPOUND CODE	BINDING SCORE
M1	-7.39
M2	-7.27
M3	-7.52
M4	--8.13
M5	-7.51
M6	-7.53
M7	-8.05
M8	-7.28
M9	-7.44
M10	-7.65
M11	-8.00
M12	-8.87
M13	-8.04
M14	-7.74
M15	-7.74
M16	-7.77
M17	-7.89
M18	-8.14
M19	-8.00
M20	-7.89
M21	-7.31
M22	-7.84
M23	-7.57
M24	-7.18
M25	-7.04
M26	-8.90
M27	-7.63
M28	-7.50
M29	-7.98
M30	-8.11
LINEZOLID	-8.13

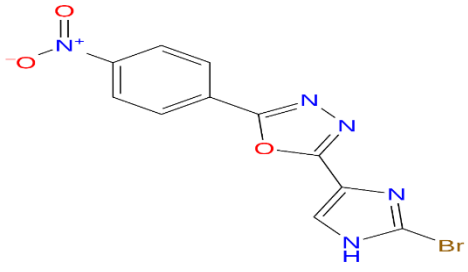
Molecular docking results for designed compounds using 3SRQ

COMPOUND CODE	BINDING SCORE
M1	-7.19
M2	-7.35
M3	-7.95
M4	-7.74
M5	-7.73
M6	-7.33
M7	-8.77
M8	-7.51
M9	-7.39
M10	-7.29
M11	-7.94
M12	-8.18
M13	-8.61
M14	-7.92
M15	-7.92
M16	-8.10
M17	-8.21
M18	-8.81
M19	-7.74
M20	-8.17
M21	-7.00
M22	-7.91
M23	-7.91
M24	-7.25
M25	-7.45
M26	-9.44
M27	-7.36
M28	-7.53
M29	-7.55
M30	-7.44
LIINEZOLID	-8.50

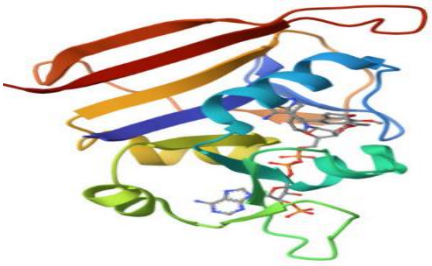
Analysis of molecular docking:



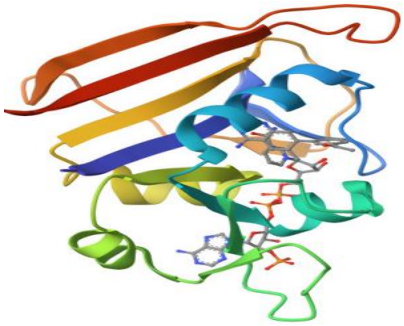
M26 – 3FY8



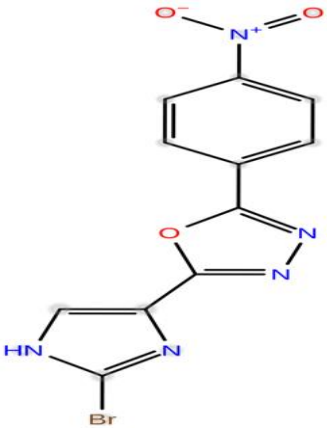
M26 – 3SRQ



FY8



3SR(

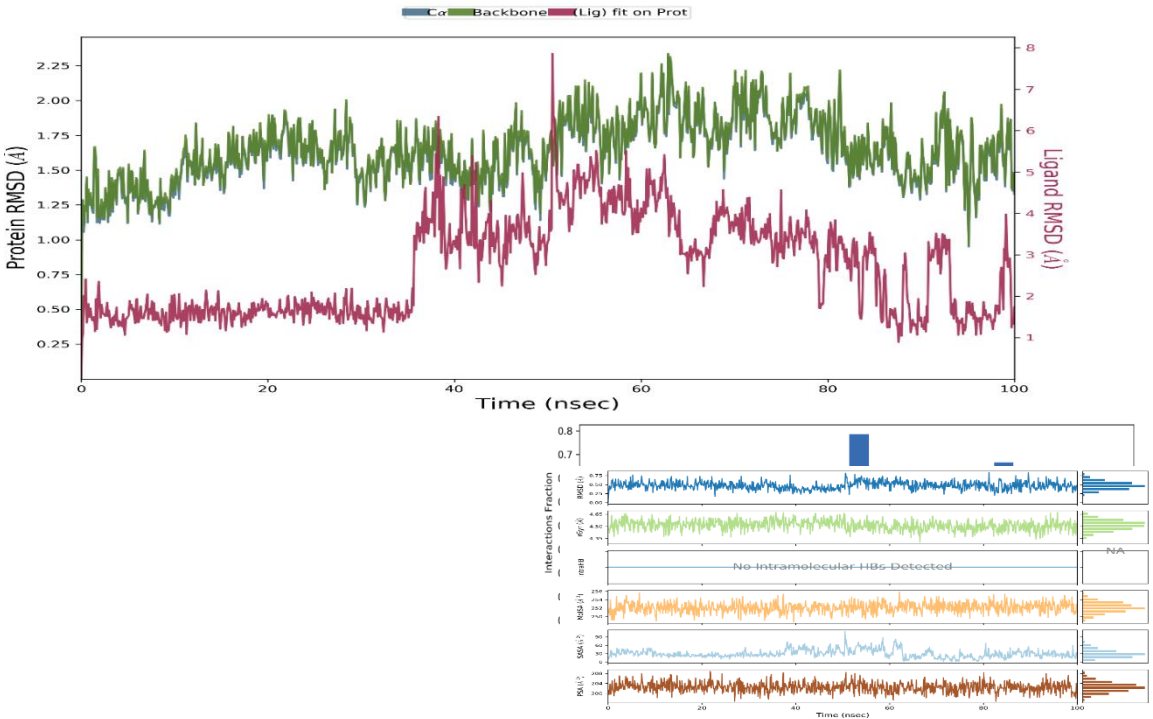


MD simulations:

A molecular dynamics (MD) simulation was performed using Desmond v5.9 (Schrödinger, LLC) to elucidate the influence of the solvent environment on the conformational dynamics and stability of the protein–ligand complex. The Optimized Potentials for Liquid Simulations (OPLS-4) force field was employed to describe the atomic interactions within the system, following the protocol outlined in the referenced literature. The docked complex was positioned at the geometric center of an orthorhombic simulation box, ensuring an optimal spatial configuration for periodic boundary conditions. To mimic a physiological aqueous environment, the simulation box was solvated using the TIP3P explicit water model, maintaining a 10 Å buffer distance between the protein surface and the box boundaries to prevent artefactual interactions between periodic images. The system volume was subsequently optimized based on the complex type and solvation requirements. To achieve electrostatic neutrality and maintain ionic strength, counterions (Na^+ and Cl^-) were randomly introduced into the solvent environment. Following system construction, the energy minimization step was carried out to eliminate steric clashes and optimize the initial geometry, ensuring a physically realistic starting configuration for the MD production run. The final simulation was conducted under NPT ensemble conditions (constant number of particles, pressure, and temperature), thereby replicating near-physiological thermodynamic states. A representative experimental compound derived from the 1,3,4-oxadiazole scaffold was selected for this analysis to validate the computational protocol and assess the reliability of the simulation outcomes. The trajectory data were subsequently analyzed to evaluate parameters such as root mean square deviation (RMSD), root mean square fluctuation (RMSF), radius of gyration (Rg), and hydrogen bonding patterns, which collectively provide insights into the structural stability, conformational flexibility, and binding persistence of the complex throughout the simulation timescale.

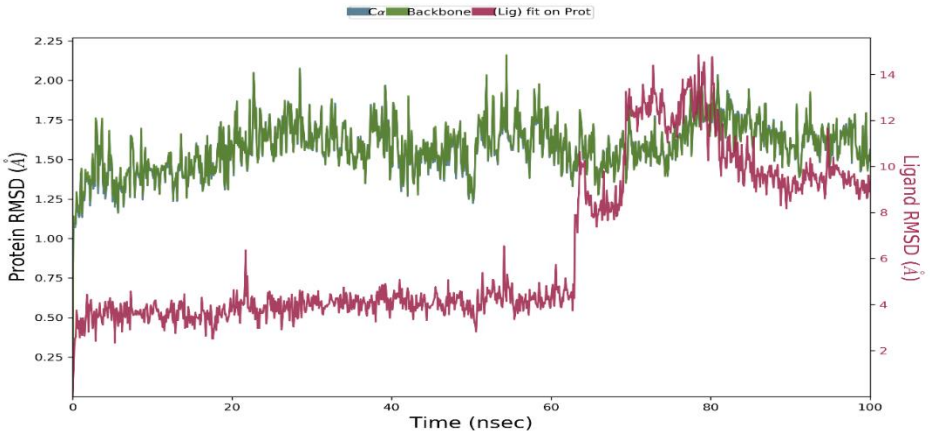
Molecular Dynamic Study of Compound (M26)

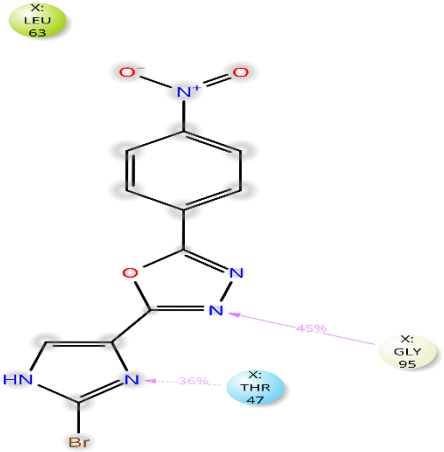
Root-mean-square deviation (RMSD) graph of the compound M26 during MD simulation

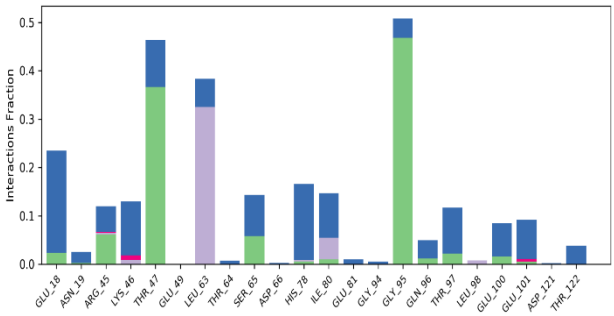


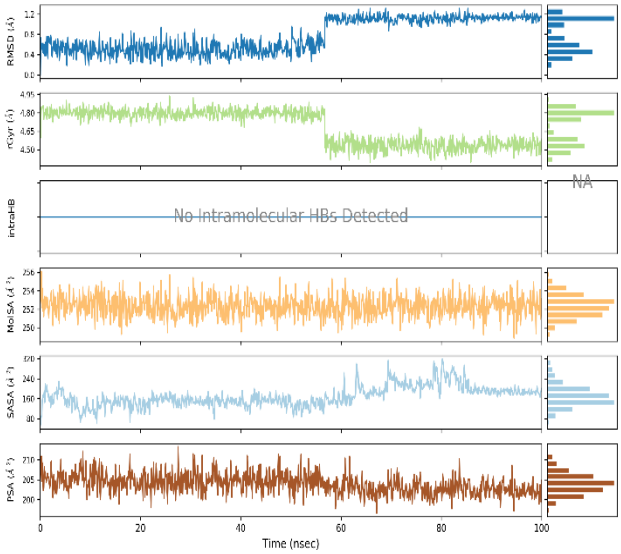
Molecular Dynamic Study of Compound (M26)

Root-mean-square deviation (RMSD) graph of the compound M26 during MD simulation









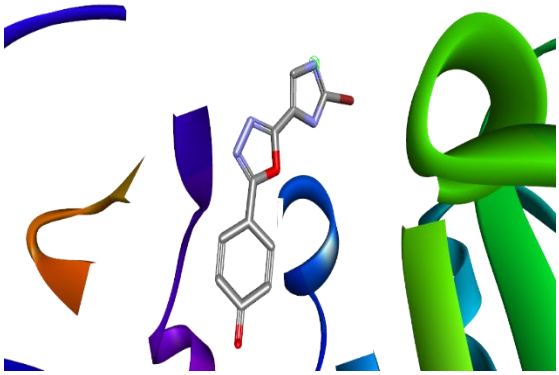
Molecular docking interaction for D6 compound of 3FY8 PDB

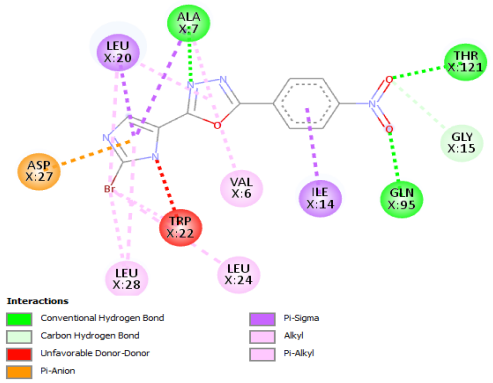
Compound	Binding affinity	Interaction residue	Type of interaction	Distance
M26	-8.90	ALA7	Conventional H bonding	1.83316
		GLN95	Carbon H bonding	1.96479
		THR121	Pi-Anion	2.05254
		GLY15	Pi-Sigma	3.70036

Molecular docking interaction for D6 compound of 3SRQ PDB

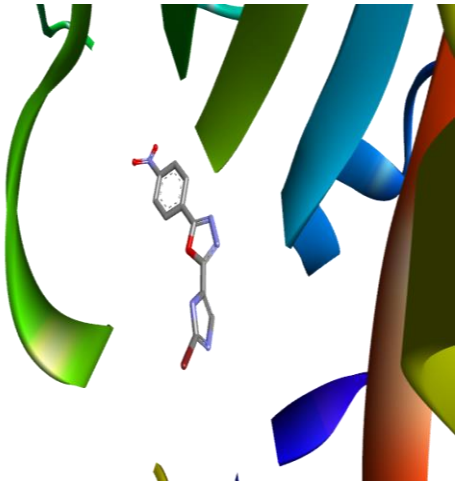
Compound	Binding affinity	Interaction residue	Type of interaction	Distance
M26	-9.44	ARG45	Conventional H- Bond	2.26187
		LYS46	Pi- Donor	2.70192
		THR64	Pi-Sigma	1.86449
		SER65	Pi-Alkyl	1.70114
		GLY95	Pi-Pi	2..07914

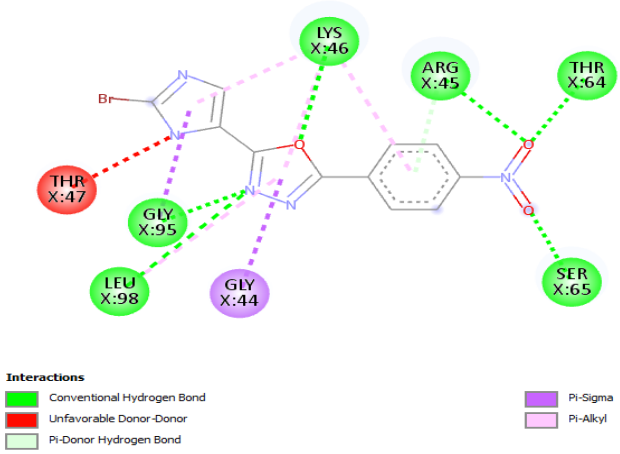
2D and 3D representation of M26 compound of 3FY8 PDB





2D and 3D representation of M26 compound of 3SRQ PDB





3. Conclusion

In this QSAR investigation, the original dataset was transformed into a numerical form using a comprehensive set of molecular descriptors, leading to the development of a statistically robust, stable, and predictive model. The successful establishment of this model provides a valuable framework for exploring descriptor contributions toward the inhibition of the transpeptidase enzyme. Both internal and external validation parameters confirmed the model's reliability and predictive capacity, as evaluated through statistical indices generated by the employed chemoinformatics software. The validated model was subsequently applied to a set of newly designed analogs to predict their potential bioactivity against the target enzyme. To further substantiate the QSAR findings, molecular docking analyses were conducted on the top-ranked predicted active compounds, providing insights into their structural complementarity and interaction profiles within the active site of the transpeptidase enzyme. Among these, compounds M26 and M27 (note: you repeated M26 twice earlier; likely one should be M27) exhibited the most favorable docking scores, −8.90 and −9.44 kcal/mol, respectively, indicating a strong binding affinity toward the target and suggesting their potential as highly potent transpeptidase inhibitors. These results highlight their significance as lead molecules that may contribute to the development of next-generation antibacterial therapeutics. Pharmacokinetic evaluation through in silico ADME (Absorption, Distribution, Metabolism, and Excretion) profiling further supported the drug-like nature of the designed compounds. All molecules satisfied Lipinski's Rule of Five parameters—molecular weight, hydrogen bond donors and acceptors, partition coefficient (log P), and molar refractivity—indicating favorable oral bioavailability and physicochemical properties. The compounds also met additional drug-likeness criteria, such as Veber's and Ghose's rules, confirming their potential suitability for further optimization and advancement into preclinical evaluation. Collectively, these results demonstrate that the designed 1,3,4-oxadiazole derivatives possess desirable pharmacodynamic and pharmacokinetic characteristics, reinforcing their candidacy as promising transpeptidase enzyme inhibitors with potential therapeutic relevance.

Acknowledgements:

The authors would like to thank the Management of Santhiram College of Pharmacy and School of Pharmacy SBV Chennai Campus for their support and encouragement.

Conflict of interest:

The Authors declared no conflict of interest in this article.

Authors' Contributions:

All authors contributed to data analysis, drafting, and revising of the paper and agreed to be responsible for all the aspects of this work.

Funding:

No funding was received to assist with the preparation of this article.

Ethical approval:

There is no ethical approval in this article.

References

Stollé, R. Ueber Die Ueberführung Der Secundären Säurehydrazide in Derivate Des Furodiazols, Pyrrodiazols Und Thiodiazols. *Berichte Dtsch. Chem. Gesellschaft* 1899, *32*, 797–798.

Hetzheim, A.; Möckel, K. Recent Advances in 1,3,4-Oxadiazole Chemistry. *Adv. Heterocycl. Chem.* 1967, *7*, 183–224.

Patel, K.D.; Prajapati, S.M.; Panchal, S.N.; Patel, H.D. Review of Synthesis of 1,3,4- Oxadiazole Derivatives. *Synth. Commun.* 2014, *44*, 1859–1875.

D. Oliveira, C.S.; Lira, B.F.; Barbosa-Filho, J.M.; Lorenzo, J.G.F.; de Athayde-Filho,

P.F. Synthetic Approaches and Pharmacological Activity of 1,3,4-Oxadiazoles: A Review of the Literature from 2000–2012. *Molecules* 2012, *17*, 10192–10231.

Boström, J.; Hogner, A.; Llinàs, A.; Wellner, E.; Plowright, A.T. Oxadiazoles in Medicinal Chemistry. *J. Med. Chem.* 2012, *55*, 1817–1830.

Banerjee, A.G.; Das, N.; Shengule, S.A.; Srivastava, R.S.; Shrivastava, S.K. Synthesis, Characterization, Evaluation and Molecular Dynamics Studies of 5, 6-Diphenyl-1,2,4- Triazin-3(2 H)-One Derivatives Bearing 5-Substituted 1,3,4-Oxadiazole as Potential Anti-Inflammatory and Analgesic Agents. *Eur. J. Med. Chem.* 2015, *101*, 81–95.

Gulnaz, A.R.; Mohammed, Y.H.E.; Khanum, S.A. Design, Synthesis and Molecular Docking of Benzophenone Conjugated with Oxadiazole Sulphur Bridge Pyrazole Pharmacophores as Anti Inflammatory and Analgesic Agents. *Bioorg. Chem.* 2019

Abd-Ellah, H.S.; Abdel-Aziz, M.; Shoman, M.E.; Beshr, E.A.M.; Kaoud, T.S.; Ahmed,

A.S.F.F. New 1,3,4-Oxadiazole/Oxime Hybrids: Design, Synthesis, Anti- Inflammatory, COX Inhibitory Activities and Ulcerogenic Liability. *Bioorg. Chem.* 2017, *74*, 15–29.

Jayashankar, B.; Lokanath Rai, K.M.; Baskaran, N.; Sathish, H.S. Synthesis and Pharmacological Evaluation of 1,3,4-Oxadiazole Bearing Bis(Heterocycle) Derivatives as Anti-Inflammatory and Analgesic Agents. *Eur. J. Med. Chem.* 2009, *44*, 3898–3902.

Kaur, J.; Soto-Velasquez, M.; Ding, Z.; Ghanbarpour, A.; Lill, M.A.; van Rijn, R.M.; Watts, V.J.; Flaherty, D.P. Optimization of a 1,3,4-Oxadiazole Series for Inhibition of Ca^{2+}/Calmodulin-Stimulated Activity of Adenylyl Cyclases 1 and 8 for the Treatment of Chronic Pain. *Eur. J. Med. Chem.* 2019, *162*, 568–585.

Tantray, M.A.; Khan, I.; Hamid, H.; Alam, M.S.; Dhulap, A.; Kalam, A. Synthesis of Benzimidazole-Linked-1,3,4-Oxadiazole Carboxamides as GSK-3β Inhibitors with in Vivo Antidepressant Activity. *Bioorg. Chem.* 2018, *77*, 393–401.

Singh, P.; Sharma, P.; Sharma, J.; Upadhyay, A.; Kumar, N. Synthesis and Evaluation of Substituted Diphenyl-1,3,4-Oxadiazole Derivatives for Central Nervous System Depressant Activity. *Org. Med. Chem. Lett.* 2012, *2*, 8.

Yadagiri, B.; Gurrala, S.; Bantu, R.; Nagarapu, L.; Polepalli, S.; Srujana, G.; Jain, N. Synthesis and Evaluation of Benzosuberone Embedded with 1,3,4-Oxadiazole, 1,3,4- Thiadiazole and 1,2,4-Triazole Moieties as New Potential Anti Proliferative Agents. *Bioorg. Med. Chem. Lett.* 2015, *25*, 2220–2224.

Glomb, T.; Szymankiewicz, K.; Świątek, P. Anti-Cancer Activity of Derivatives of 1,3,4-Oxadiazole. *Molecules* 2018, *23*, 3361.

Shyma, C.P.; Balakrishna, K.; Peethambar, K.S.; Vijesh, M.A. Synthesis, Characterization, Antidiabetic and Antioxidant Activity of 1,3,4-Oxadiazole Derivatives Bearing 6-Methyl Pyridine Moiety. *Scholars Research Library Der Pharma Chemical* 2015, *7*, 137–145.

Nazreen, S.; Alam, M.S.; Hamid, H.; Yar, M.S.; Shafi, S.; Dhulap, A.; Alam, P.; Pasha, M.A.Q.; Bano, S.; Alam, M.M.; et al. Design, Synthesis, in Silico Molecular Docking and Biological Evaluation of Novel Oxadiazole Based Thiazolidine-2,4-Diones Bis-Heterocycles as PPAR-γ Agonists. *Eur. J. Med. Chem.* 2014, *87*, 175–185.

Şahin, G.; Palaska, E.; Ekizoğlu, M.; Özalp, M. Synthesis and Antimicrobial Activity of Some 1,3,4-Oxadiazole Derivatives. *Farmaco* 2002, *57*, 539–542.

Ali, M.A.; Shaharyar, M. Oxadiazole Mannich Bases: Synthesis and Antimycobacterial Activity. *Bioorg. Med. Chem. Lett.* 2007, *17*, 3314–3316. [Google Scholar] [CrossRef]